RESEARCH PAPER

Characterization of Low Temperature Plasma Ion Nitriding (PIN) of Inconel 600 and 601 Alloys

R. Kumar[1*], Y. Chandra Sharma[2], V. V. Sagar[3] and D. Bhardwaj[1]

* ravindrauniversal@yahoo.com

[1] Birla Institute of Technology, Mesra, Jaipur Campus, India..

[2] Vivekananda Global University, Jaipur, India .

[3] Malviya National Institute of Technology, Jaipur, India.

Abstract: *IIn this study an effort has been made for the plasma ion nitriding (PIN) of Inconel 600 and 601 alloys at low temperatures. After plasma ion nitriding and microstructural study, growth kinetics of nitrided layer formation and wear properties were investigated by various characterization techniques such as scanning electron microscope (SEM), X-ray diffraction (XRD) analysis, micro-hardness measurement and wear test by pin on disk technique. It was found that surface micro-hardness increases after the PIN process. A mixed peak of epsilon (ε) and fcc (γ) phase was detected for all temperature range (350 to 450 0C), while the chromium nitride (CrN) phase was detected at elevated temperature range ~450 0C in Inconel 601 alloy. The calculated values of the diffusion coefficient and activation energy for the diffusion of nitrogen are in accordance with the literature. Volume loss and wear rate of the plasma nitrided samples decreases, but it increases as PIN process temperature increases.*

Keywords: *Micro-hardness; X-ray diffraction; Wear test; Diffusion coefficient; Plasma nitriding.*

1. INTRODUCTION

Ni-base alloys are widely used material for various applications such as; chemical processing plants, gas turbines, heat exchanger, and nuclear industries due to excellent corrosion resistance and resistance to heat properties. Inconel 600 and 601 alloys have excellent properties but show poor wear resistance, low surface hardness, and a high coefficient of friction [1]. These disadvantages can be improved by surface modification. Many surface modification processes such as diffusion processes (nitriding, carburizing, boriding etc.) and coating processes (CVD, PVD, PECVD etc.) have been tried by various researchers [2–7]. Pulsed DC plasma ion nitriding is a diffusion process and the most promising technique to improve the surface properties of Ni and Fe based alloys, because it has excellent dimensional control, low distortion, environment friendliness and complete process is auto control [8]. It is a thermochemical process in which nitrogen is introduced into the metal surface as an interstitial solid solution [8].

Plasma nitriding of pure iron (Fe) and Fe based alloys has been thoroughly explained by various researchers [9–14] but very little information on nickel-based alloys is available in the literature. Williamson et al. [15] studied that, when Ni-Fe alloys are exposed to low energy, high current density nitrogen ion beam the nitriding affinity reduced with the increasing of Ni concentration. Pedraza et al. [16] reported that Ni and Ni-Cr based alloys form thinner nitrided layer compared to Fe based alloys when these were nitrided under the ion implantation technique. Aw et al. [17] studied the plasma nitriding behavior of Inconel 718 alloy at temperature range 550 to 750 °C for 16h treatment time. In this study it was found that the time and temperature were not effective to increase the nitrided layer thickness. Mindivan et al. [18] studied the wear performance of Inconel 600 by different nitriding processes, it was concluded that wear rate is lower for the pulsed plasma nitrided samples, but the nitriding processes did not significantly affect the surface hardness of such alloy. Aw et al. [19] reported the friction and wear behavior of plasma nitrided Inconel 718 alloy and demonstrated that the hard nitrided layer reduces the friction coefficient of the material. It was also concluded that the layer was prone to delimitation under contact motion resulting in the higher wear rate, i.e. a thicker nitrided layer was required to

achieve improved tribological properties. Sudha et al. [20] studied the nitriding kinetics of Inconel 600 alloy, it was found that surface hardness increased from 200 to 1260 VHN after plasma nitriding at 600 °C for 24 h. The calculated value of activation energy for the diffusion of nitrogen was obtained as 0.65 eV. Sun [21] studied the layer growth kinetics during plasma nitriding of Inconel 600 alloy, it was concluded that the growth of the nitrided layer with temperature deviates from conventional diffusion law. It was also concluded that the nitrided layer follows two linear regimes, in a fast-growth regime the growth of the nitrided layer was governed by nitrogen diffusion in the layer. On the other hand in slow-growth regime nitrogen diffusion in the developed external scale governs the kinetics of nitrided layer growth. Some other studies on nitriding behavior of Ni-based alloys and Ni–Cr based composites under various experimental conditions have been reported by various workers [1, 22-28].

The existing information available in the literature was insufficient to understand the behavior of nitrided layer growth and wear properties at a low- temperature range. Therefore, the present work was focused to investigate the properties of Inconel 600 and 601 alloys at a lower temperature range ~350 - 450 °C after pulsed dc plasma ion nitriding. All the experiments were performed in Nitrogen (N_2) and Hydrogen (H2) gas environment at the ratio of N_2-H_2 (50-50) % at three different temperatures (350, 400, and 450 °C). After plasma nitriding, samples were characterized by various characterization techniques such as; scanning electron microscope (SEM), X-ray diffraction (XRD) analysis, micro-hardness measurement, and wear test by pin on disk method.

2. SAMPLE DETAILS AND PREPARATION

Samples used for assessment were commercially available Inconel 600 and 601 alloys. The chemical compositions of these standard Inconel alloys are given in Table 1. Circular disc-shaped samples of two sizes: 15mm diameter x 20mm thickness prepared for SEM, XRD analysis and hardness measurement, and 10mm diameter x 10mm thickness sample prepared for wear testing. Initially, samples were polished with SiC emery papers of 240, 320, 400, 600, 800 grit size followed by a diamond paste of 1 μm grain size and alumina paste of 0·05 μm grain size. After polishing, the samples were washed with acetone for removal of dust/oil contamination from the surface and finally dried.

3. PLASMA NITRIDING EXPERIMENTAL SET-UP

The schematic diagram of the experimental set-up for plasma ion nitriding has been shown in Fig 1. The main components of the experimental setup are; vacuum pump, gas cylinders, mass flow controllers (MFC), pulsed dc power supply, and thermocouple.
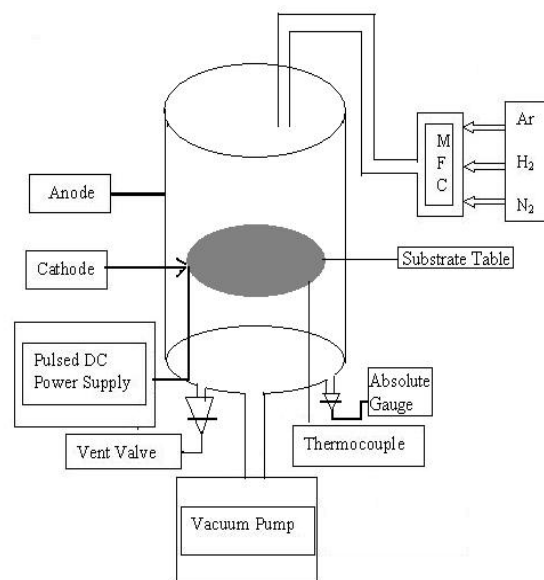

Fig.1. Plasma nitriding experimental setup.

Initially the chamber was evacuated up to the base pressure of ~5x10^{-3} mbar with the help of a rotary pump. After that Argon (Ar) and Hydrogen

Table 1: Chemical compositions in wt% of selected Inconel alloys.

Steel grade	Cr	Ni	Mn	Si	Al	Fe
Inconel 600	15.5	75.5	0.20	0.30	00	8.5
Inconel 601	23	60.5	0.25	0.45	1.4	14.4

Table 2: Plasma nitriding process parameters.

Gas Pressure	4 mbar
Gas Ratio (N$_2$: H$_2$)	50:50 (%)
Applied Voltage	620 Volts
Nitriding Time	4 hours
Temperature	350 ^{0}C, 400 ^{0}C, 450 ^{0}C

(H$_2$) gases were introduced into the chamber having a volume ratio of 50% Ar and 50% H$_2$ to maintain a gas pressure of 1 mbar which was measured by an absolute gauge. At this gas pressure, initially a glow discharge plasma was ignited between the chamber wall as anode and substrate table as a cathode by applying pulsed dc voltage of ~400 Volts at ~30 kHz frequency. This Ar-H$_2$ discharge was utilized to remove the oxides and contaminants from the sample surface. After an hour, N$_2$-H$_2$ gases were introduced into the chamber in a volume ratio of 50% N$_2$ and 50% H$_2$ through mass flow controllers (MFC). A typical working gas pressure of ~4 mbar was maintained for carrying out the plasma nitriding process. A thermocouple was used to measure the sample temperature. The typical plasma nitriding operating parameters are given in Table 2.

4. RESULTS AND DISCUSSION

4. 1. Micro-Hardness Measurement and Analysis of Surface Morphology

Fig. 2 shows the variation in surface micro-hardness with plasma nitriding process temperatures. The surface micro-hardness was observed to increase as process temperature increases. Initially, it is observed that the surface micro-hardness increases slowly up to the process temperature of 400 ^{0}C, while beyond this temperature range the surface micro-hardness increases rapidly in both the alloys. The maximum surface micro-hardness ~306 HV and ~330 HV were observed in Inconel 600 and 601 alloys, respectively. The increments in the surface hardness value after plasma nitriding from its initial surface hardness value (200-220 HV) were due to the formation of nitride phase during plasma nitriding at the surface.
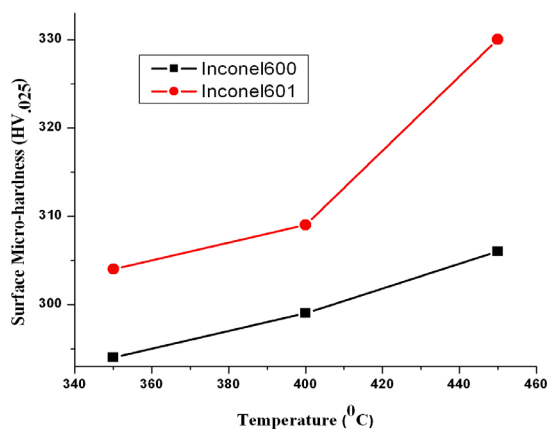

Fig. 2. Variation of surface micro-hardness with plasma nitriding temperature.

Sudha et al. [20] observed ~900 VHN surface micro-hardness in Inconel 600 alloy after nitriding at temperature 450 ^{0}C for 24 hours. It was also observed that surface hardness remain the same till 500^{0}C, beyond which it increased further with increasing temperature. Mindivan et al. [18] observed very slight changes in surface hardness when Inconel 600 alloy was plasma nitrided at 520 ^{0}C for 12 hours. Figs. 3 and 4 show the surface morphology images of Inconel 600 and 601 alloys, before and after plasma nitriding at different process temperatures.
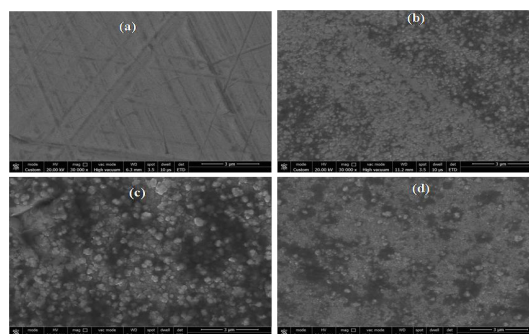
Fig. 3. SEM surface morphology of Inconel 600 alloy (a) untreated sample. (b) plasma nitrided at 350 ^{0}C. (c) plasma nitrided at 400 ^{0}C. (d) plasma nitrided at 450 ^{0}C.
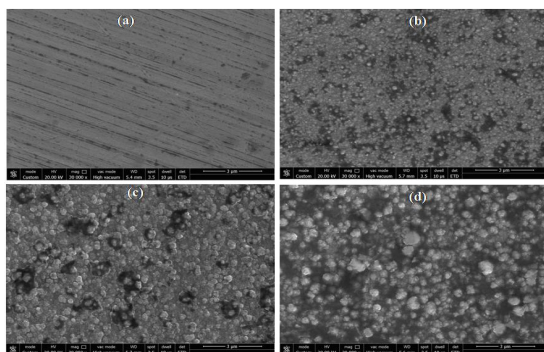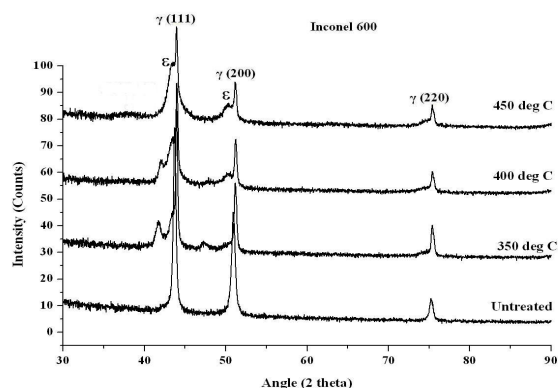
Fig. 4. SEM surface morphology of Inconel 601 alloy
(a) untreated sample. (b) plasma nitrided at 350 ^{0}C.
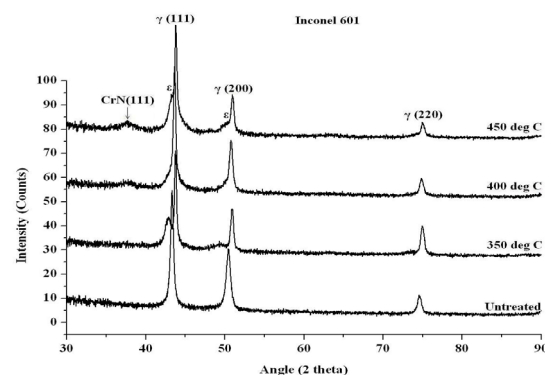(c) plasma nitrided at 400 ^{0}C. (d) plasma nitrided at 450 ^{0}C.

Fig. 5. Comparison of the XRD pattern of Inconel 600 alloy before and after plasma nitriding.

Fig. 6. Comparison of the XRD pattern of Inconel 601 alloy before and after plasma nitriding.

The average crystallite size of 5-9 nanometers was roughly calculated using the Scherrer formula [29] after plasma nitriding. In this calculation, peak broadening due to microstrains and instrumental broadening was not taken into consideration. It was observed from surface morphology images, the crystallite size increased as process temperature increased. Sudha et al. [20] calculated CrN crystallite size around 10nm after plasma nitriding for 24 h at 600 ^{0}C.

4.2. Identification of Phase Composition in the Nitrided Layer

The results of X-ray diffraction analysis of Inconel 600 and Inconel 601 are shown in Figs 5 and 6. The untreated sample shows only the fcc (γ) phase corresponding to the Ni-Fe-Cr based matrix. After plasma nitriding an additional peak appeared at a position of 2θ (37.50) which was identified as chromium nitride CrN phase in (111) plane. This CrN peak was observed only in the samples of Inconel 601 alloys which were plasma nitrided at 450 ^{0}C. A mix peak of epsilon (ε) phase with fcc (γ) phase of (111) and (200) planes at the 2θ position of 41.620, 43.280, and 51.140 were observed in all the plasma nitrided samples for all temperatures (350-450 ^{0}C). Sun [21] suggested that this mix peak may be resulted due to the formation of a thermodynamically unstable compound of ε-Ni$_3$N or (Ni, Cr, Fe, Mn)3N1-x in the nitrided layer. It has been known that ε-Ni$_3$N is unstable under normal pressure and formed only at high nitrogen potentials [30].

The characteristic of mixed peak formation during plasma nitriding was not observed in the study by Sudha et al. [20] and Mindivan et al. [18] for Inconel 600 alloy. The observed γ peaks were found to be asymmetric and broad in the plasma nitrided samples as compared to untreated samples. The peak broadening in the plasma nitrided samples were related to the development of stress in the sample matrix due to the diffusion of nitrogen.

4.3. Growth Kinetics of Nitrided Layer

Figs. 7 and 8 show the cross-sectional micrographs of the plasma nitrided samples of Inconel 600 and 601 alloys obtained from a scanning electron microscope. The obtained micrograph shows the variation in the thickness of the nitrided layer with nitriding temperatures 350, 400 and 450 ^{0}C.
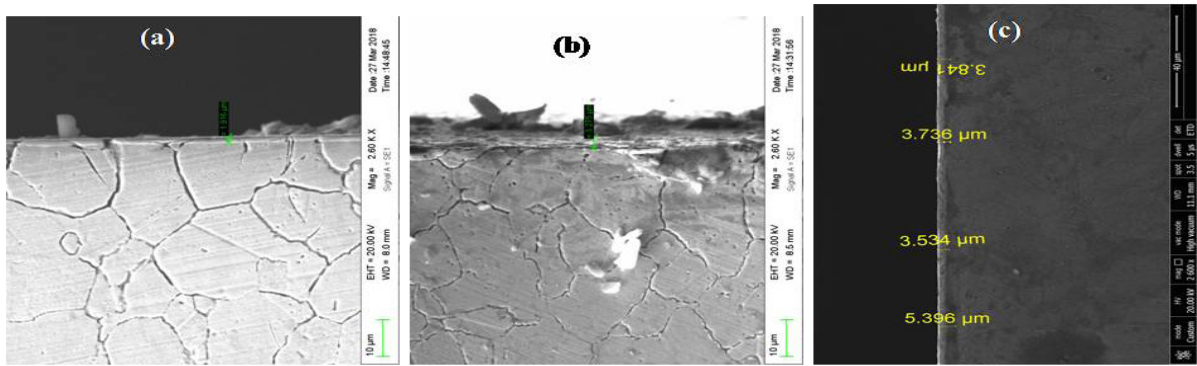
Fig.7. SEM image of plasma nitrided layer of Inconel 600
(a) plasma nitrided at 350 ^{0}C. (b) plasma nitrided at 400 ^{0}C. (c) plasma nitrided at 450 ^{0}C.
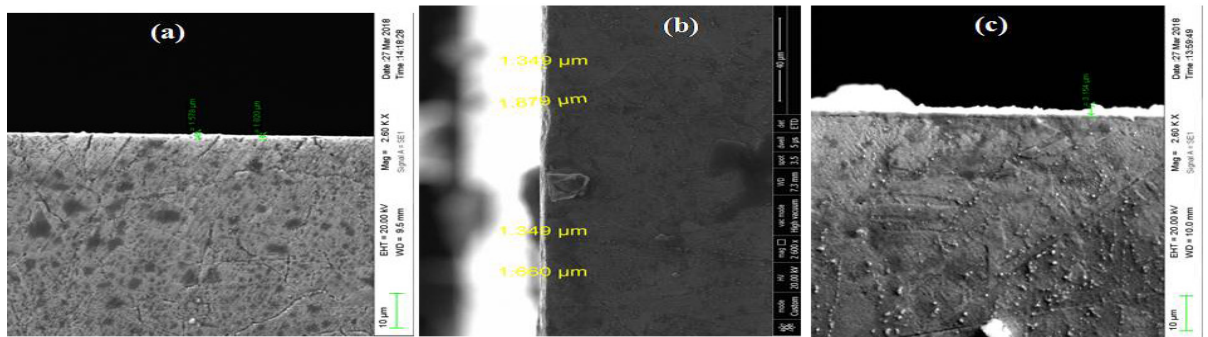
Fig. 8. SEM image of plasma nitrided layer of Inconel 601
(a) plasma nitrided at 350 ^{0}C. (b) plasma nitrided at 400 ^{0}C. (c) plasma nitrided at 450 ^{0}C.

It was observed that the thickness of the nitrided layer increases in both the alloys as plasma nitriding process temperature increases. The maximum thickness of the nitrided layer ~3.70 µm and ~3.15 µm were observed in Inconel 600 and 601 alloys respectively. It was also observed that at 450 ^{0}C nitrided layer is divided into two sub-layers. The existence of the formation of a double layer structure in the nitriding of Ni-Cr alloys was reported in the literature [23, 31]. Sun [21] observed a ~7µm thick nitride layer for 5h nitriding and ~11µm thick nitride layer for 12h nitriding at 450 ^{0}C. It was also observed that the further increment in the nitriding temperature led to a reduction in nitrided layer thickness. The temperature of 500-600 ^{0}C did not affect the layer thickness. Sudha et al. [20] observed a ~14µm thick nitride layer for nitriding at a temperature of 600 ^{0}C for 24h. In this study it was also observed that the layer thickness increased with increasing time for all nitriding temperatures 450-600 ^{0}C, but for longer treatment time increase in layer thickness was steeper than for shorter treatment time. Mindivan et al. [18] observed a 7 µm thick nitride layer for 12h nitriding at 520 ^{0}C.

Further, to understand the influence of plasma nitriding process parameters, the thickness of the nitrided layer was plotted as a function of plasma nitriding process temperature, as shown in Fig 9. Thickness was taken as the total nitrided layer (addition of sub-layers in case of the plasma of the samples nitrided at 450 ^{0}C).
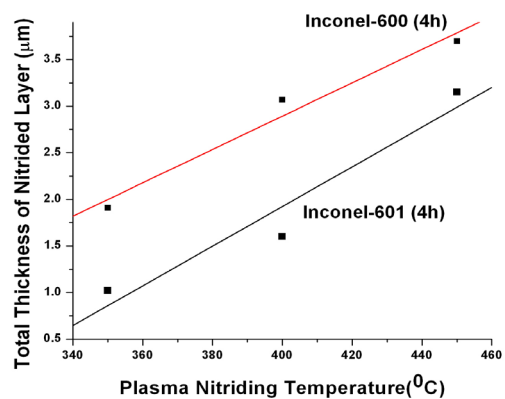
Fig. 9. Variation in the total thickness of the plasma nitrided layer of Inconel 600 and 601 alloys with different plasma nitriding temperatures.

Fig. 9 shows that the thickness of the nitrided layer increases linearly with increasing plasma nitriding process temperature. As per the theory of diffusion in solids, the thickness of the nitrided layer 'X' is related to the nitriding time 't' through the following relation written as in equation (1) [32].

$$X = \sqrt{(D_N \cdot t)} \tag{1}$$

Here; 'D_n' is the diffusion coefficient of nitrogen, which was related to the activation energy 'Q' and the pre-exponential term 'D_0' by a relation written as in equation (2) [32].

$$D_n = D_0 \exp\left(-\frac{Q}{RT}\right) \tag{2}$$

Or

$$\ln(D_n) = \ln(D_0) - \frac{Q}{RT} \tag{3}$$

Here; 'D_0' is the pre-exponential term and 'Q' is the activation energy, 'R' is the gas constant 8.62×10^{-5} eV/atom^{-K}, and 'T' is the absolute temperature. Using the measured values of nitrided layer thickness from SEM images for nitriding time duration 4h, values of diffusion coefficient 'D_n' were calculated by Equation (1), within the temperature range of 350 ^{0}C - 450 ^{0}C. The value of D_n varies from 2.5×10^{-16} m^2/s to 9.5×10^{-16} m^2/s and 7.2×10^{-17} m^2/s to 6.8×10^{-16} m^2/s for Inconel 600 and 601 alloys respectively. Using Equation (3) $\ln(D_n)$ V$_s$ reciprocal of temperature (1/T) were plotted in fig 10.

From this fig the values for activation energy 'Q' were calculated ~1.21 eV and ~1.24 eV for Inconel 600 and 601 alloys. Sudha et al. [20] reported that the value of activation energy was 0.65 eV for Inconel 600 alloy. Leroy et al. [23] obtained the value of diffusion coefficient of nitrogen ~10^{-15} m^2/s and activation energy ~1.1 eV at 400 ^{0}C in Inconel 690 alloy. Matsuda et al. [33] reported the diffusion coefficient of nitrogen ~8×10^{-16} m^2/s and activation energy ~0.43 eV at 650 ^{0}C in Ni-20 wt.% Cr-2 wt.% Ti alloy. In another study made by Kodentsov et al. [34] reported values of diffusion coefficient of nitrogen ~1.8×10^{-16} m^2/s and activation energy ~1.5 eV at 600 ^{0}C in Ni-5 at.% Cr alloy. On the other hand the similar calculated values of activation energy for the diffusion of nitrogen are presented by Sun [35] for the plasma carburizing kinetics of AISI 316L and AISI 304L stainlests steels and Menthe and Rie [36] for the plasma nitriding of AISI 304L steel. It is to be noted that all the nickel alloys and steels having high Cr and Ni contents, which explains the similarity of the activation energy values. The higher value of activation energy and the linear behavior of plasma nitriding thickness as a function of the square root of treatment time indicate that the whole process is controlled by the diffusion of the nitrogen atom in the layer.

4.4. Wear Analysis of Plasma Nitrided Samples

Wear test was performed on these alloys by the pin on disk method to analyze the wear properties. This test was performed in the dry condition with a 10N applied load. After the wear test mass loss was measured using three digits balancing machine. Using the values of mass loss, volume loss was calculated by using the well-known relation between mass, density, and
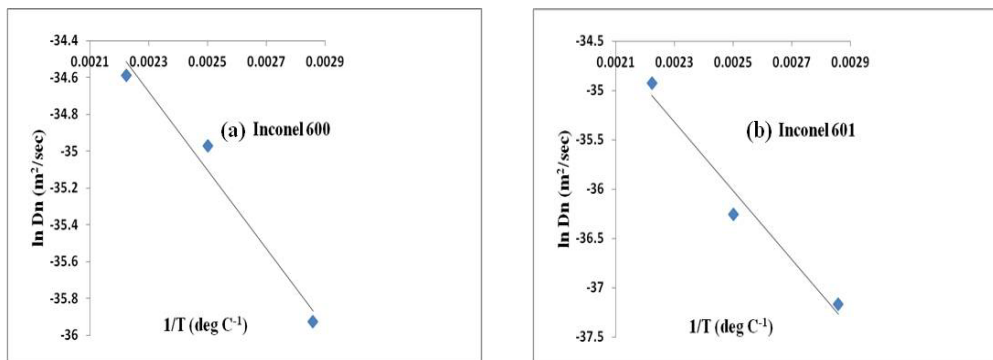

Fig. 10. Arrhenius plot of logarithmic of diffusion coefficient vs reciprocal of temperature (a) for 600 alloy and (b) for 601 alloy.

Table 3: Volume loss of Inconel 600 and 601 alloys before and after plasma nitriding.

Temperature	Volume Loss (cm³)	
	Inconel-600	Inconel-601
Untreated	8.26×10^{-3}	5.67×10^{-3}
350 ^{0}C	2.12×10^{-3}	2.8×10^{-3}
400 ^{0}C	5.78×10^{-3}	4.43×10^{-3}
450 ^{0}C	9.68×10^{-3}	8.38×10^{-3}

volume. The calculated values of volume loss for both the alloys have reported in Table 3. It is evident that, the volume loss decreases after plasma nitriding. The minimum volume loss $\sim$2.12 x 10^{-3} cm^3 and $\sim\sim$2.8 x 10^{-3} cm^3 observed in the samples which were plasma nitrided at 350 ^{0}C. The volume loss was found to increase with increasing nitriding temperature. It was also revealed that, at 450 ^{0}C volume loss exceeded in nitrided samples as compared to untreated samples for both the alloys.

Using the values of volume loss, calculated wear rate was calculated by using the following relation given in equation (4).

Wear rate = Volume loss /(Sliding distance x Load)   (4)

For the fixed value of the sliding distance (2000m), values of wear rate (mm^3/Nm) obtained have been shown in Fig. 11.
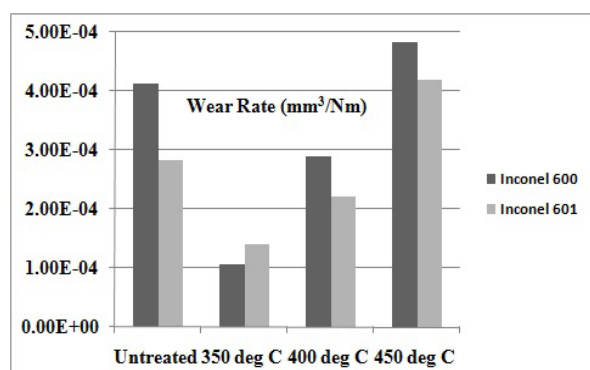
Fig. 11. Wear rate (mm^3/Nm) of untreated and plasma nitrided samples of Inconel 600 and 601.

The minimum wear rates $\sim$1.06 x 10^{-4} mm^3/Nm and $\sim$1.4 x 10^{-4} mm^3/Nm were found for the samples of Inconel 600 and 601 alloys which

were nitrided at 350 ^{0}C respectively. The wear rate was found to increase with increasing nitriding temperature. At 450 ^{0}C the wear rate exceeded $\sim$4.84 x 10^{-4} mm^3/Nm and $\sim$4.19 x 10^{-4} mm^3/Nm as compared to untreated samples $\sim$4.13 x 10^{-4} mm^3/Nm and $\sim$2.83 x 10^{-4} mm^3/Nm for both the alloys. It is also observed that the increase of wear rate is fast in the Inconel 601 alloy as compared to Inconel 600 alloy. It may be related to the formation of a thin hard phase (CrN) at the surface of the Inconel 601 alloy at this particular temperature (450 ^{0}C). The thin hard CrN phase has the brittle nature that increases the wear rate. Kahraman et al. [37] reported that the samples which were nitrided for 10 h duration show maximum wear resistance due to the formation of thick compound and diffusion layer as compared to the samples which have a thin compound layer.
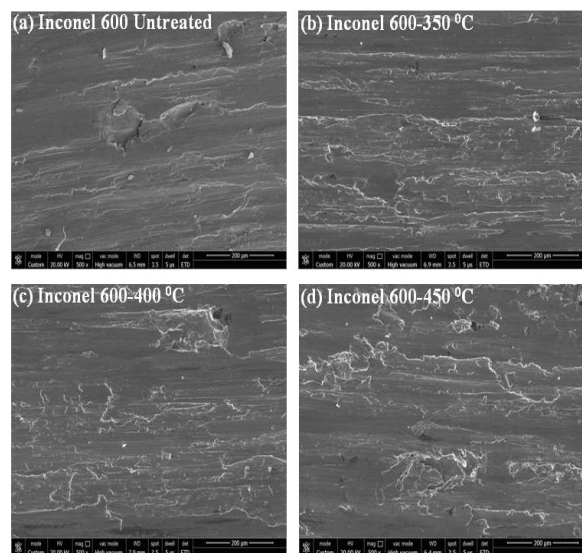
Fig. 12. SEM image of untreated and plasma nitride samples of Inconel 600 alloy after wear test.
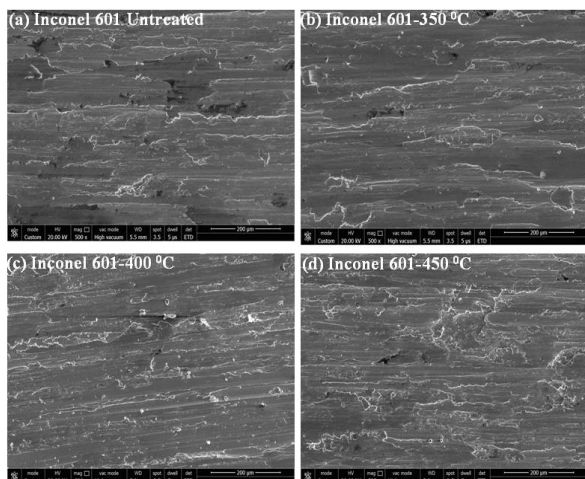
Fig. 13. SEM image of untreated and plasma nitride samples of Inconel 601 alloy after wear test

5. CONCLUSIONS

Based on this study following conclusions can be drawn:

1. Plasma nitriding of Inconel 600 and 601 alloys at a temperature between 350 to 450 ^{0}C can produce a thin nitrided layer ~3.15 μm and ~3.70 μm. The thickness of the nitrided layer increases as nitriding temperature increases.

2. Surface microhardness was found to increase after plasma nitriding. It increases slowly up to 400 ^{0}C. The maximum surface micro-hardness ~306 HV and ~330 HV were observed at 450 ^{0}C in Inconel 600 and 601 alloys respectively.

3. CrN Phase was not detected in Inconel 600 alloy for all temperature range (350 – 450 ^{0}C). However, CrN Phase was detected in Inconel 601 samples that were plasma nitrided at 450 ^{0}C only. A mix peak of the epsilon (ε) phase with the γ phase of (111) and (200) planes were observed in all the nitrided samples for all temperature range 350 to 450 ^{0}C.

4. The values of diffusion coefficients ~9.5 x 10^{-16} m^2/s and ~6.8x10^{-16} m^2/s and the values of activation energy for the diffusion of nitrogen ~1.21 eV and ~1.24 eV were obtained for Inconel 600 and 601 alloys respectively. The whole process was seemed thermally activated and the growth of the nitrided layer was controlled by the diffusion of the nitrogen atom.

5. The volume loss and wear rate were found to decrease after the plasma nitriding process. The minimum wear rate ~1.06 x 10^{-4} $mm^3/$Nm and ~1.4 x 10^{-4} mm^3/Nm were found in the samples of Inconel 600 and 601 alloys, which were nitrided at 350 ^{0}C. The SEM images agreed with the trends of our calculated values of wear rate with some anomaly.

6. ACKNOWLEDGMENT

REFERENCES

1. Dahm, K. L., Short, K. T. and Collins, G. A., "Characterization of nitrogen-bearing surface layers on Ni-base super alloys." Wear, 2007, 263, 625-628.

2. Ueda, N., Mizukoshi, T., Demizu, K., Sone, T., Ikenaga, A. and Kawamoto, M., "Boriding of nickel by the powder-pack method." Surface and Coatings Technology, 2000, 126, 25-30.

3. Singh, V. and Meletis, E. I., "Synthesis, characterization, and properties of intensified plasma-assisted nitrided super alloy." Surface & Coatings Technology, 2006, 201,1093.

4. Sitek, R., Sikorski, K., Sobczak, J. and Wierzcho, T., "Structure and properties of the multilayers produced on Inconel 600 by the PACVD method with the participation of trimethyl aluminum vapors." Materials Science-Poland, 2008, 26, 767.

5. Borowski, T., Brojanowska, A., Kost, M., Garbacz, H. and Wierzchon., T., "Modifying the properties of the Inconel 625 nickel alloy by glow discharge assisted nitriding." Vacuum, 2009, 83, 1489-1493.

6. Espallargasa, N. and Mischler, S., "Dry wear and tribocorrosion mechanisms of pulsed plasma nitrided Ni–Cr alloy." Wear, 2011, 270, 464-471.

7. Sista, V., Kahvecioglu, O., Kartal, G., Zeng, Q. Z., Kim, J. H., Eryilmaz, O. L. and Erdemir, A., "Evaluation of electrochemical boriding of Inconel 600."

Surface and Coatings Technology, 2013, 215, 452-459.

8. David Pye, "Practical Nitriding and Ferritic Nitro-carburizing." ASM International, Materials Park, Ohio (2003).

9. Leigh, S., Samandi, M., Collins, G. A., Short, K. T., Martin, P. and Wielunski, L., "The influence of ion energy on the nitriding behavior of austenitic stainless steel." Surface and Coatings Technology, 1996, 85, 37-43.

10. Menthe, E. and Rie, K. T., "Further investigation of the structure and properties of austenitic stainless steel after plasma nitriding." Surface and Coatings Technology, 1999, 116–119, 199-204.

11. Kumar, S., Baldwin, M. J., Fewell, M. P., Haydon, S. C., Short, K. T., Collins, G. A. and Tendys, J., "The effect of hydrogen on the growth of the nitrided layer in r.f. plasma nitrided austenitic stainless steel AISI 316." Surface and Coatings Technology, 2000, 123, 29-35.

12. Hosseini, S. R. and Ashrafizadeh, F., "Accurate measurement and evaluation of the nitrogen depth profile in plasma nitrided iron." Vacuum, 2009, 83, 1174-1178.

13. Udyavar, M. and Young, D. J., "Precipitate morphologies and growth kinetics in the internal carburization and nitridation of Fe–Ni–Cr alloys." Corros. Sci., 2000, 42, 861-883.

14. Manova, D., Mandl, S., Neumann, H. and Rauschenbach, B., "Influence of grain size on nitrogen diffusivity in austenitic stainless steel." Surface and Coatings Technology, 2007, 201, 6686-6689.

15. Williamson, D. L., Davis, J. A. and Wilbur, P. J., "Effect of austenitic stainless steel composition on low-energy, high-flux, nitrogen ion beam processing." Surface and Coatings Technology, 1998, 103–104, 178-184.

16. Pedraza, F., Reffass, M., Abrasonis, G., Savall, C., Riviere, J. P., Dinhut, J. F., "Low-energy High-flux Nitriding of Ni and Ni20Cr Substrates." Surface and Coatings Technology, 2004, 176, 236-242.

17. Aw, P. K., Batchelor, A. W. and Loh, N. L., "Structure and tribological properties of plasma nitrided surface films on Inconel 718." Surface and Coatings Technology, 1997, 89, 70–76.

18. Mindivana, F. and Mindivan, H., "Comparisons of wear performance of hardened Inconel 600 by different nitriding processes." Procedia Engineering, 2013, 68, 730 – 735.

19. Aw, P. K., Batchelor, A. W. and Loh, N. L., "Failure mechanisms of plasma nitrided Inconel 718 film." Wear, 1997, 208, 226–236.

20. Sudha, C., Anand, R., Thomas Paul, V., Saroja, S. and Vijayalakshmi, M. "Nitriding kinetics of Inconel 600." Surface and Coatings Technology, 2013, 226, 92–99.

21. Sun, Y., "Kinetics of layer growth during plasma nitriding of nickel-based alloy Inconel 600." Journal of Alloys and Compounds, 2003, 351, 241–247.

22. Rizk, A. and Saad, G., "The effects of ion bombardment on the surface hardening of Inconel 625 in D.C. glow discharges." Surface and Coatings Technology, 1980, 11, 415-420.

23. Leroy, C., Czerwiec, T., Gabet, C., Belmonte, T. and Michel, H., "Plasma assisted nitriding of Inconel 690." Surface and Coatings Technology, 2001, 142–144, 241-247.

24. Borowski, T., Brojanowska, A., Kost, M., Garbacz, H. and Wierzchon, T., "Modifying the properties of the Inconel 625 nickel alloy by glow discharge assisted nitriding." Vacuum, 2009, 83, 1489-1493.

25. Singh, V. and Meletis, E. I., "Synthesis, characterization and properties of intensified plasma-assisted nitrided superalloy Inconel 718." Surface and Coatings Technology, 2006, 201, 1093-1101.

26. Makishi, T. and Nakata, K., "Surface hardening of nickel alloys by means of plasma nitriding." Metall. Mater. Trans-A, 2004, 35A, 227-238.

27. Eliasen, K. M., Christiansen, T. L. and Somers, M. A. J., "Low temperature gaseous nitriding of Ni-based superalloys." Surf. Eng., 2010, 26, 248-255.

28. Zhao, J., Peng, X., Wang, Y. and Wang, F., "Plasma nitridation of a novel Ni–10.8 wt% Cr nanocomposite." Acta Mater., 2007, 55, 3193-3201.

29. Ahmad M., Mohammad R. F. and Mohammad R. M., "Modified Scherrer Equation to Estimate More Accurately Nano-Crystallite Size Using XRD." World Journal of Nano Science and Engineering, 2012, 2, 154-160.

30. Wriedt, H. A., "The N – Ni (nitrogen – nickel) system." Bull. Alloy Phase Diagram, 1985, 6, 558-563.

31. Dong, H., "S-phase surface engineering of Fe-Cr, Co-Cr and Ni-Cr alloys." Int. Mater. Rev., 2010, 55, 65-98.

32. Callister W. D., "Materials Science and Engineering, An Introduction." John Willy & Sons, 2007.

33. Matsuda, F., Nakata, K., Makishi, T. and Kiya, S., "Surface hardening of Ni alloys by means of Plasma Ion Nitriding (PIN) process." Trans. JWRI, 1988, 17, 127-136.

34. Kodentsov, A. A., Van Dal, M. J. H., Cserhati, C., Daroczi, L. and Van Loo, F. J. J., "Permeation of nitrogen in solid nickel and deformation phenomenon accompanying internal nitridation." Acta Mater., 1999, 47, 3169-3180.

35. Sun Y., "Kinetics of low temperature plasma carburizing of austenitic stainless steels." Journal

of Materials Processing Technology, 2005, 168, 189-194.

36. Menthe, E. and Rie, K. T., "Further investigation of the structure and properties of austenitic stainless steel after plasma nitriding." Surface and Coatings Technology. 1999, 116-119, 199-204.

37. Kahraman, F. and Karadeniz, S., "Characterization and Wear Behavior of Plasma Nitrided Nickel-Based Dental Alloy." Plasma Chemistry Plasma Process, 2011, 31, 595-604.